Theoretical and Applied Climatology (2025) 156:164
https://doi.org/10.1007/s00704-025-05359-5

RESEARCH

Spatio-temporal trends in daily precipitation extremes over the Enkangala escarpment of South Africa: 1961–2021

Hadisu Bello Abubakar[1,2] · Mary C. Scholes[1] · Francois A. Engelbrecht[2]

Received: 27 May 2024 / Accepted: 7 January 2025

Abstract

The Intergovernmental Panel on Climate Change in its Sixth Assessment Report reported that increases in extreme weather events can already be detected in every region in the world. For eastern southern Africa the report provides evidence of an increasing trend in extreme precipitation events, but more research is needed to understand how this change is manifesting over regions as diverse as South Africa's eastern escarpment and northern Mozambique. This study evaluates the trends in extreme precipitation over the Enkangala Escarpment, part of South Africa's eastern escarpment, over the period 1961 to 2021. Daily precipitation data covering 22 stations with fewer than 10% missing values over 61 years were obtained from the South African Weather Service. A total of twelve extreme events precipitation indices were computed using the ClimPACT2 package, and a time series trend analysis was performed using the Trend Free Whitening Mann Kendal test and a field significance test. The results indicate significant increasing trends in nine out of the twelve extreme events indices that were investigated. The three indices which have shown significant decreasing trends include Consecutive Wet days (CWD) at (0.03 day/year total annual rainfall (PRCPTOT) (0.61 mm/decade) and the annual count of days when precipitation≥10 mm (R10mm) of 0.32 days/decade. Indices such Rx1 days, Rx3 days and Rx5 days exhibited increasing trends of 0.2 days/decade each. Other indices with an increasing trend are CDD (3.6 day/decade), R20mm (0.2 days/decade) and R30mm (0.2 days/decade). The R95p (11.2 mm/decade) and R99p (6.0 mm/decade) indices, and Simple Daily Intensity Index(0.4 mm/decade) also exhibit positive trends over the study period. Overall the analysis is indicative of a change in the nature of rainfall over the Enkangala escarpment of South Africa, with annual rainfall totals, the number of consecutive wet days and the frequency of events with smaller thresholds such as 10 mm/day decreasing, but with extreme events of larger thresholds occurring more frequently. That is, when it rains, it tends to rain more intensely than in the past. The use of a field significance test was useful to formalise when relatively small but spatially homogeneous trends detected at separate weather stations yield statistical significance. The findings of the paper are relevant to decision and policy in multiple of socio-economic sectors active in South Africa's eastern escarpment.

1 Introduction

Southern African has been identified as a climate change hotspot in the Intergovernmental Panel on Climate Change (IPCC) Special Report on Global Warming of 1.5 °C (Hoegh-Guldberg et al. 2018, 2019). This stems from the region being projected to become drastically warmer, and likely also generally drier, under low mitigation climate change futures (Engelbrecht et al. 2009, 2015; Ranasinghe et al. 2021; Hoegh-Guldberg et al. 2018). Given that the region's climate is already warm and water-stressed (Engelbrecht and Engelbrecht 2016), such a change implies that opportunities for adaptation are limited (which is essentially what renders the region a climate change hotspot) (Engelbrecht and Monteiro, 2022). Extreme events such as tropical

✉ Hadisu Bello Abubakar
guidenet80@gmail.com; 1364152@students.wits.ac.za

Mary C. Scholes
Mary.Scholes@wits.ac.za

Francois A. Engelbrecht
Francois.Engelbrecht@wits.ac.za

[1] School of Animal, Plant and Environmental Sciences, University of the Witwatersrand, Private Bag X3, Johannesburg 2050, South Africa

[2] Global Change Institute, University of the Witwatersrand, Private Bag X3, Johannesburg 2050, South Africa

Published online: 18 February 2025

cyclone Idai, that hit Mozambique in 2019, the 2015/16 summer rainfall drought in southern Africa and Durban Flood of 2022 are three of the most costly events in southern Africa over the past five decades, costing the economy billions of $US via the damages incurred (Douris and Kim 2021).

South Africa's eastern escarpment is important in terms of both rain-fed and irrigation agriculture (Strauss et al. 2021; Olabanji et al. 2020), forestry (Naidoo et al. 2013) and biodiversity (Nel et al. 2017). This area is critical to South Africa's water security where rainfall totals are relatively high (Engelbrecht et al. 2002), and where its large dams are located (Taylor et al. 2016; Engelbrecht and Monteiro, 2022). However, over this part of South Africa, projected rainfall futures are uncertain, in the sense that there is no model agreement in terms of the direction of the change (Lee et al. 2021). There is therefore clear value in understanding observed climate trends in this region, also in terms of changes in extremes.

Several studies have explored historical rainfall trends over southern Africa (Kruger and Sekele 2013; MacKellar et al., 2014; Bruinsma 2017; Naidoo 2022) and based on these the IPCC assessed that rainfall totals over the region have been decreasing in recent decades (Ranasinghe et al. 2021). This decreasing trend can be detected in the summer rainfall regions of western and eastern southern Africa, as well as in the winter rainfall region of South Africa (Ranasinghe et al. 2021). However, the IPCC assessed that extreme rainfall events have been increasing in frequency in recent decades over eastern southern Africa (including South Africa's eastern escarpment), despite the decline in rainfall totals (Ranasinghe et al. 2021). This finding has recently been confirmed for a century-long data set covering 1921–2020 (McBride et al., 2022).

In this paper, we explore in some detail the observed trends in extreme precipitation over the Enkangala escarpment, which forms the central part of South Africa's eastern escarpment. We focus on this region given its importance for agriculture, forestry and water security in South Africa's economy (Nhemachena et al. 2020; Branca et al. 2021). The Enkangala escarpment forms part of South Africa's larger summer rainfall region, and most of the rainfall that occurs in this region is convective. The thunderstorms that bring the bulk of rainfall to the Enkangala escarpment can cause heavy falls of rain, hail, damaging winds, tornadoes and lightning (Punge et al. 2023; Bopape et al. 2022; Sierks 2022). Intense convective rainfall events are also important for the region in terms of their ability to produce runoff and eventually streamflow (Yin et al. 2021; Quintero et al. 2022), and on the negative side, in terms of their ability to cause soil erosion and possible flooding (Zhao et al. 2021; Ran et al. 2019; Dunkerley 2021). In a warmer global climate, general increases in the intensity of precipitation are projected due to the atmosphere's ability to hold more water vapor (Trenberth 2011; Gu et al. 2017). However, regional changes in circulation and moisture transport may also decrease water vapour concentrations even in the presence of temperature increases.

Our study consequently explores the hypothesis that the well-documented warming in southern Africa (Engelbrecht et al. 2015; Ranasinghe et al. 2021) is associated with an increase in intense precipitation over the Enkangala escarpment. Investigating spatiotemporal extreme precipitation trends is important to inform adaptation interventions. Although the previously mentioned studies have explored precipitation trends over eastern South Africa, site-specific studies analyzing rainfall characteristics in the Enkangala Escarpment have not been conducted. Here we explore the local statistical significance of trends in extreme precipitation indices in several locations in the Enkangala escarpment. Additionally, we make use of a field significance test, to explore when a spatial coherency in rainfall trends that are locally insignificant, may still yield a statistically significant change over an encompassing area.

2 Materials and methods

2.1 Study area

The Enkangala Escarpment is part of the greater Drakensberg region found in the eastern Escarpment of South Africa (Fig. 1). It is a biodiversity hotspot with a dense network of headwaters of rivers (Tugela, Pongola, Usutu, and Vaal) and their watersheds. The Enkangala escarpment is defined here as an area of 2 ° in latitude by 2 ° in longitude (approximately $200 \times 200 km^2$), with the northwest corner located at 26.965 S; 28.991 °E and a southeast corner at 28.791 S, 30.908 °E. The Escarpment supports agriculture, forestry, and hydropower generation, which are vital for the bioeconomy of South Africa (Anekwe et al. 2023). It excludes the high Drakensberg along the KwaZulu Natal-Lesotho border that provides water to the Tugela system, as well as the integrated Vaal River system that provides water to South Africa's Gauteng province via inter-basin water transfers (Taylor et al. 2016). The major biophysical changes are as result of land use change in the form of agricultural activities; and additionally there is also rapid urbanization taking place in the area, (Onaolapo et al. 2022).

While the altitude in the Enkangala Escarpment ranges from 166 to 3242 m, the weather stations available for this study spanned an altitudinal range from 1050 at Elandslaagte to 1852 m at Tygerfontein. The Enkangala Escarpment region identified above is important for South Africa's

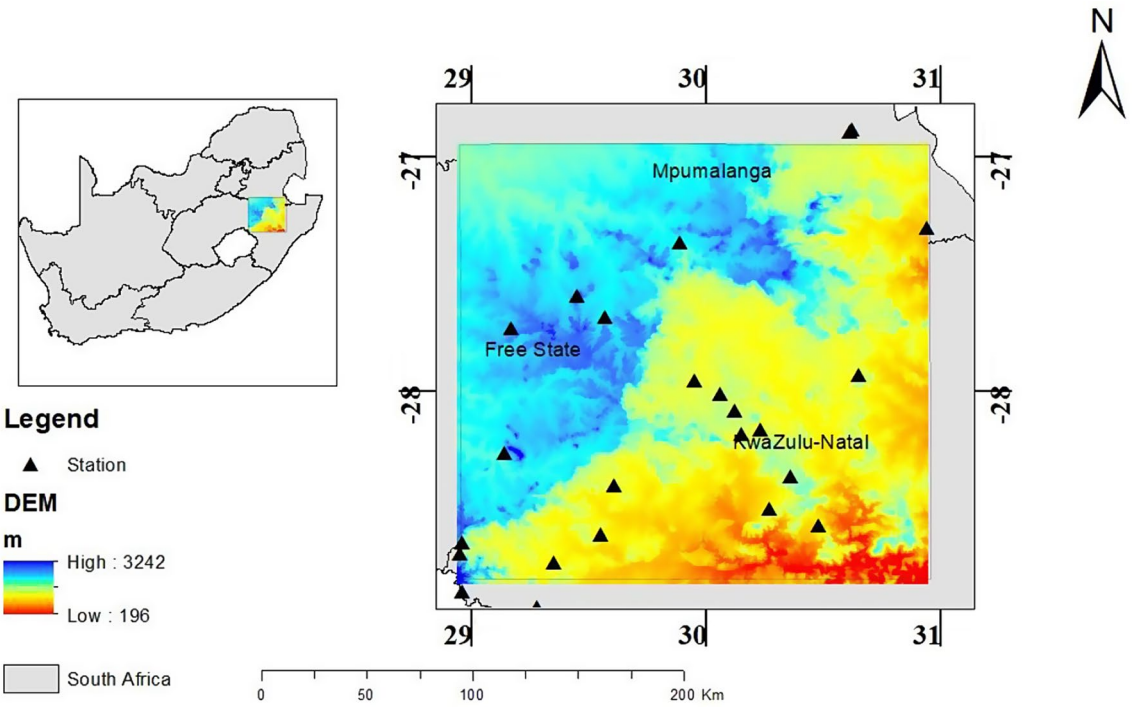

Fig. 1 Topography of the Enkangala Escarpment and the location of the 22 weather stations operated by the South African Weather Service (SAWS), which are found in the provinces of Free State, Mpumalanga, and KwaZulu-Natal

water security, as well as for local rain-fed agriculture. Identifying rainfall trends for this region is therefore important.

2.2 Data sources and quality assurance

Daily rainfall totals for 22 high-quality stations were obtained from the South African Weather Service (SAWS), for the period 1961 to 2021 (Fig. 1), out of a larger set of 69 stations, where stations with more than 30 days of missing data were excluded. Within the records used, missing data were replaced based on nearby stations. When 1 or 2 days were missing, the average of neighbouring stations for the same days was used. Missing data for consecutive days were calculated with the long-term average of the same days from different years. These stations also met the criteria of having less than 10% missing values for the period of interest.

The data quality was checked using the Climatol package in R (Guijarro 2018; Guijarro et al. 2023), to locate precipitation values, including outliers that likely exist because of errors rather than from unlikely physical events. A crucial step in quality control is testing for homogeneity of the time-series, because of discrepancies that may occur independently from the climate, including broken instruments, modifications/upgrades to instrumentation, changes in station exposure and location, changes in observational procedures, and changes in aggregation methods. The Climatol package offers efficient dataset control for outlier discovery and correction and can define break points (Guijarro 2014, 2018, 2019) while homogenising the series.

Climatol software uses relative homogenisation procedures, which are more robust than absolute procedures since they incorporate values from the correlated neighbouring stations (Guijarro et al. 2023). Based on their weighted average, Climatol generates a single composite reference series from the participating stations. The series is normalised, and missing values of the original data are filled in together with the outliers. The operation is split into an optimal iterative process to achieve stability of the series, and the series statistical properties (mean and standard deviation) are recalculated—the stability of the mean leads to the normalisation of the data. Using the composite reference series values, the missing values are weighted with the available values from the stations of their cluster. Table 1 lists the indices used in this study to identify extreme events. Table 2 in Sect. 3 below provides the list of stations considered here.

2.3 Methodology

Multi-decadal (1961–2021) trends were examined, in several extreme rainfall statistical indices for the Enkangala Escarpment, using the Trend Free Pre-Whitening Mann-Kendall test (TFPWMK) and statistical significance was applied (Bartolini et al. 2022; Garba and Abdourahamane 2023; van der Walt and Fitchett 2021; Montero-Martínez and Andrade-Velázquez 2022).

Table 1 Provides detailed information about those indices (type, indices, description, definitions, and units) used to evaluate extreme rainfall between 1961 and 2021 over the Enkangala Escarpment using the ClimPACT2. RR is the daily precipitation sum

Type	Indices	Description name	Definition	Units
Duration indices	CDD	Consecutive dry days	Maximum number of consecutive days when RR < 1 mm	Days
	CWD	Consecutive wet days	Maximum number of consecutive days when RR ≥ 1 mm	Days
	SDII	Simple daily intensity index	Annual total precipitation divided by the number of wet days (defined as precipitation ≥ 1.0 mm) in a year	mm/day
Absolute Indices	Rx1day	Max 1-day precipitation amount	Monthly maximum 1-day precipitation	mm
	Rx3day	Max 3-day precipitation amount	Monthly maximum consecutive 3-day precipitation	mm
	Rx5day	Max 5-day precipitation amount	Monthly maximum consecutive 5-day precipitation	mm
Percentile-based indices	R95P	Very wet days	Annual total precipitation when daily precipitation > 95th percentile	mm
	R99P	Extremely wet days	Annual total precipitation when daily precipitation > 99th percentile	mm
Threshold indices	R10mm	Number of days above 5 mm	Annual count of days when precipitation ≥ 10 mm	Days
	R20mm	Number of heavy precipitation days	Annual count of days when precipitation ≥ 20 mm	Days
	R30mm	Number of very heavy precipitation days	Annual count of days when precipitation ≥ 30 mm	Days

Data analysis and mapping have been done using R 4.0.2 and Arc GIS 10.3. The spatial patterns of rainfall indices shown in the maps below were generated using inverse distance weighting (IDW) interpolation. The 12 selected indices were calculated for each weather station for the period 1961 to 2021, and subsequently spatially interpolated to a spatial grid of 0.5 resolution using the Inverse Distance Weighting (IDW) method.

2.3.1 Extreme climate indices

Climate indices were calculated using the ClimPACT2 software package, which can deal with missing data and conduct quality checks before processing the indices. The indices are recommended and developed by the WMO Commission for Climatology Expert Team on Sector-Specific Climate Indices (ET-SCI), and are accessible from https://climpact-sci.org/assets/climpact2-user-guide.pdf (Sevruk et al. 2009). Twelve precipitation indices were selected and further grouped into three classes (absolute, duration, and percentile-based indices). The Expert Team on Climate Change Detection and Indices (ETCCDI) threshold definitions are commonly used for this analysis, as recommended by the WMO (Steinschneider and Brown 2013; Palharini et al. 2021; Risser et al. 2021). We utilize the ETCCDI in this study on the Enkangala escarpment.

2.3.2 Trend-free pre-whitening mann kendall (TFPWMK)

Each rain gauge time series is presumed to be serially independent in the sense that values at a particular time are not dependent on the values at any other time. However, the results of the MK test are frequently impacted by serial correlation in the hydro-meteorological time series (Almazroui and Şen 2020; Citakoglu and Minarecioglu 2021). For instance, the significance of the MK test is understated when there is a positive (negative) serial correlation in a time series (Jin et al. 2023; Tan et al. 2020; Adeyeri et al., 2022). The TFPWMK is chosen over traditional trend analysis such MK and regression analysis due to its ability to distinguish several pre-whitening (PW) approaches, including trend-free pre-whitening, have been presented to reduce the effects of serial correlation on the MK test findings (TFPWMK). The findings of the MK test are less affected by a serial correlation within the hydro-meteorological time series when using TFPWMK (Karki et al. 2017). Therefore, TFPWMK was employed.

The initial step in TFPWMK involves normalizing the time series data by dividing each data value by the mean, removing any trends, and calculating the slope of the trend using Sen's method. After identifying and addressing any lag-1 auto-correlation, the modified individual values are then re-inserted into the original time series. The time series is reintegrated with the trend component. Subsequently, the pre-whitened time series is analysed using the MK test (Charifi Bellabas et al. 2021; Onaolapo et al. 2022; Tan et al. 2017).

Table 2 List of stations and their descriptive statistic mean annual precipitation (MAP) standard deviation (STD) and coefficient of variance (CV) over the Enkangala Escarpment, for the period between 1961–2021

Station	Latitude	Longitude	Altitude m	MAP mm	STD	CV%
Bergville	-28.73	29.35	1145	831.2	180	22
Cavern Farm	-28.64	28.96	1490	1361.4	296	22
Chelmsford Dam	-27.95	29.95	1219	812.3	175	22
Dannhauser	-28.01	30.06	1350	745.5	166	22
Dundee	-28.16	30.23	1247	795.4	203	26
Elandslaagte	-28.4	29.96	1050	762.6	180	24
Glencoe	-28.18	30.15	1311	900.2	176	20
Hattingspruit	-28.08	30.12	1310	781.3	183	23
Kingsley	-27.93	30.53	1219	682.5	166	24
Marthinusdrift	-27.52	30.73	1195	829.9	171	32
Memel	-27.68	29.57	1728	693.8	162	23
Moorside	-28.4	29.61	1219	812.4	175	22
Ncome	-27.93	30.65	1295	705.0	153	22
Newcastle	-27.73	29.92	1235	682.5	148	22
Rocco	-27.73	29.17	1844	669.7	146	22
Roseleigh	-28.61	29.55	1145	799.7	198	25
Sterkfontein	-28.41	29.04	1691	644.9	145	23
Tygerfontein	-27.59	29.45	1852	676.9	151	22
Van Reenen	-28.38	29.39	1683	976.0	186	19
Verkykerskop	-29.28	27.92	1830	670.7	143	21
Warden-SK	-27.85	28.96	1631	671.7	185	28
Warden-	-27.96	29.06	1765	701.7	135	19

2.3.3 Field significance

The significance of a trend at one or more stations may or may not be representative of the trend in the neighbouring region. The term 'field significance' describes the degree of validity of the station's trends over the surroundings. Indeed, numerous stations in each area may exhibit either positive or negative trends. Thus, regardless of the statistical significance of the individual station trends, regions with trends of a consistent sign are found using the field significance test (Zeder and Fischer 2020). The field significance of local trends can be evaluated using various techniques (Zeder and Fischer 2020; Yue and Wang 2002; Yue et al. 2003; Renard and Lang 2007). To evaluate the field significance on the escarpment. The Yue technique was used (Yue et al. 2003. This strategy bootstraps the original station network 1000 times while distorting (preserving) the auto-(cross-) correlation to prevent it from influencing the field significance analysis. Then, each site's synthetic time series is subjected to the TFPWMK test. Equation 1 has been used for each resampled network to count the sites with significant upward and downward trends at the set significance level. The area's field significance is then estimated as

$$C_f = \sum_{i=1}^{n} C_i \tag{1}$$

The value of n represents the number of stations located within a specific region under examination, while C_i denotes the tally of statistically noteworthy trends (at a significance level of 0.1) at each station, *i*. This process has been replicated 1000 times for every resampled network. The 1000 counts of significant positive (negative) trends have been ranked in ascending order utilizing the Weibull distribution (Petrow and Merz 2009). The plotting position formula yields the empirical cumulative distributions, C_f, as:

$$P\left(Cf \leq C\prime rf\right) = r/(N+1) \tag{2}$$

where *r* is the rank of *C*, and *N* is the number of resampled networks. The probability of several significant positive and negative trends in the original network has been estimated by comparing with C_f of significant positive and negative trends obtained from the resampled networks:

$$Pobs = P\left(Cf,\ obs \leq C\prime r\ f\ \right) \tag{3}$$

where *Pf* = (1*Pobs*−, for*Pobs*, *PPobsobs*≤>0.50.5).

3 Results and discussions

3.1 Temporal and spatial variability of the annual precipitation

Annual average (1961–2021) precipitation varies greatly along the Enkangala Escarpment, from 645 mm to

1361 mm, across the weather stations listed in Table 2 and depicted in Fig. 2. The highest annual average precipitation total (1361 mm) was recorded at Cavern Farm, southwest of the Enkangala Escarpment close to the Lesotho Highlands. The lowest value (643 mm) was observed at Sterkfontein Dam. These two stations are less than 50 km apart, which indicates that one must always be cautious about interpolated values for infilling of missing data.

Generally, the stations on the plateau in the northwest of the domain shown, have lower rainfall totals than those to the east or the southeast of the escarpment. The Cavern station in the southwest part of the Enkangala Escarpment has the highest standard deviation value of 296 mm per annum, with a CV of 22%.

The range of the CVs across the Enkangala Escarpment is between 19 and 32% (Table 2). This is consistent with the known high variability of rainfall over the larger eastern Drakensberg region (Dedekind et al. 2016; Engelbrecht et al. 2009; Nel and Sumner 2006; Abba and Abiodun 2017). The station with the highest CV (32%) is Marthinusdrift on the north-eastern part of the escarpment. Van Reenen and Warden Heritage, located on the central part of the Enkangala Escarpment, have the lowest CV (19%).

Seasonal rainfall is dominated by the summer December to February (DJF), September to November (SON)and autumn March to May (MAM) rainfall, which accounts on average for more than 80% of the rainfall across the Enkangala Escarpment (Fig. 3). The average range across the stations is between 236 and 695 mm for the DJF season, with winter June to August (JJA) rainfall ranging between 27.8 mm and 82.4 mm, across the stations, this cannot be seen in the figure because of the scale used. The scale was chosen to allow other seasons to be represented (Fig. 3). Clearly, the Enkangala escarpment is a region that displays pronounced dry-wet seasonality.

3.2 Interannual variation of extreme precipitation indices

The interannual variation of precipitation to extreme precipitation indices, averaged across all stations over the period 1961 to 2021 is shown in Table 2. Annual precipitation totals demonstrate pronounced interannual variability with a CV range of 19–32%, consistent with the variations listed in Table 2 for the individual stations. The following indices exhibit statistically significant ($p<0.05$) positive trends: R95p (11.2 mm/decade), R99p (6.3 mm/decade), SDII (0.4 mm/decade) and Rx1day (2.3 mm/decade). Consistently, this result is similar to regional model projections for the these indices (Pinto et al. 2016; Giorgi et al. 2014).

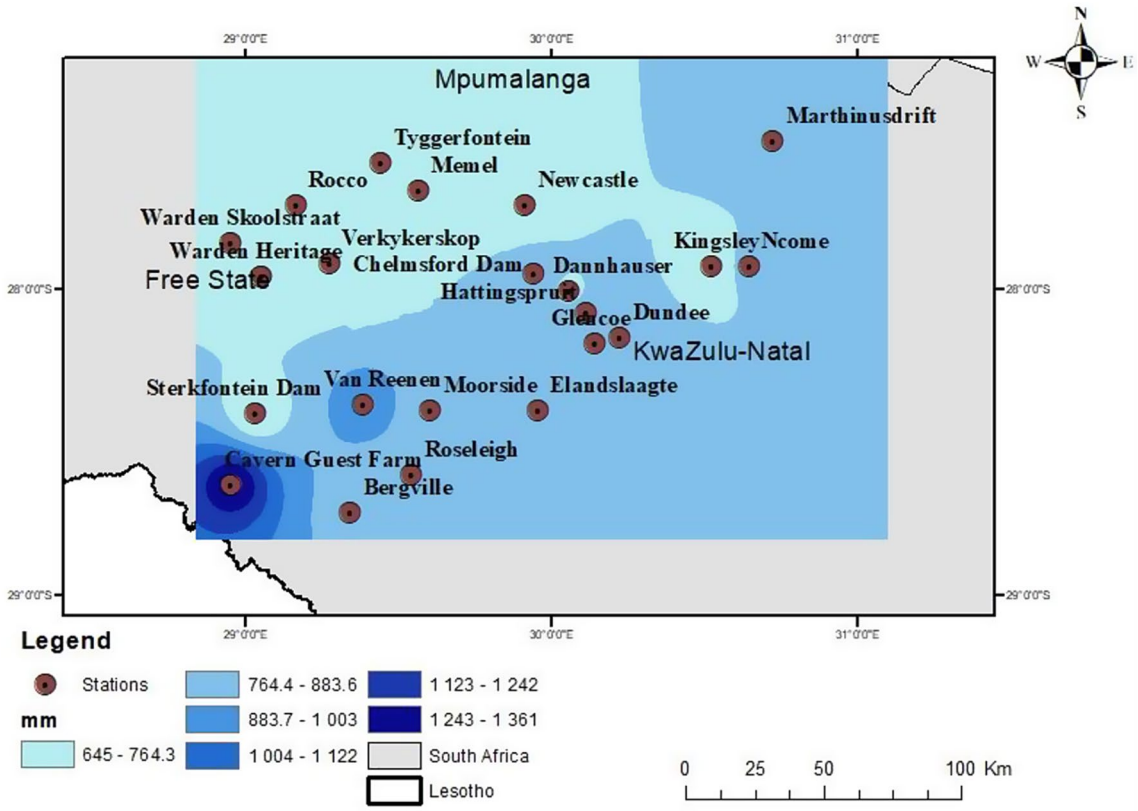

Fig. 2 Overall annual average precipitation over Enkangala Escarpment for the period 1961–2021

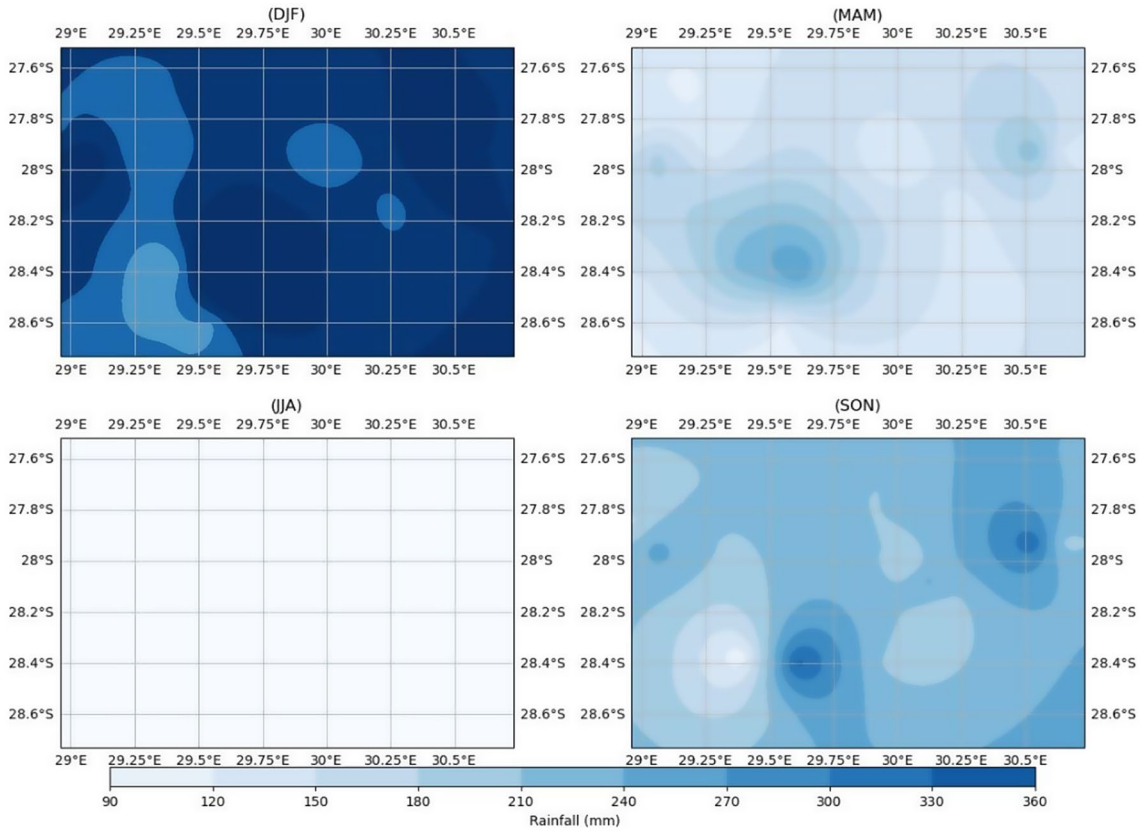

Fig. 3 The spatial distribution of mean seasonal precipitation (mm) across the Enkangala escarpment for (**A**) DJF; (**B**) MAM; (**c**) JJA; and (**D**) SON, as averaged over the period 1961–2021

Table 3 The indices, slopes and p value were calculated for the Enkangala Escarpment, for the period between 1961–2021. Note: triple stars in the significance level column stands for the 95% level of significance

Index	Slope/decade	*p*-value	Unit	sig_level
CDD	3.6	0.0542	day/year	
CWD	-0.38	0.00022	day/year	
PRCPTOT	-6.1	0.534	mm/year	
R10mm	-0.3	0.329	day/year	
R20mm	0.2	0.209	day/year	
R30mm	0.2	0.154	day/year	
R95p	11.2	0.0378	mm/year	***
R99p	6.3	0.00595	mm/year	***
Rx1day	2.3	0.00377	mm/year	***
Rx3day	1.8	0.199	mm/year	
Rx5day	1	0.531	mm/year	
SDII	0.4	0.00041	mm/year	***

Other indices have increasing trends, but without statistical significance, were also recorded for CDD (3.6 day/decade), R20mm (0.2 days/decade), 30 mm (0.2 days/decade), Rx3day (1.8 mm/decade) and Rx5day (1.0 mm/decade). The CWD index showed a significant ($p<0.05$ Table 3) decreasing trend at a rate of -0.38 mm/day/decade. During the period 1961–2021 R10mm insignificantly decreased at a rate of 0.30 days/decade.

3.3 Spatial distribution of extreme rainfall

3.3.1 Absolute indices

The spatial manifestation of the 1-day (Rx1day), 3-day (Rx3day), and 5-day (Rx5day) precipitation indices are shown in Fig. 4?. All three indices follow the same spatial distribution of average annual precipitation, with the lowest values over the plateau, with higher values to the east over the escarpment and the KwaZulu-Natal Province. In the annual mean, the intensity across the domain ranges from 46 to 100 mm for Rx1day, 75 to 140 mm for Rx3 day, and 86 to 170 mm for Rx5day (Fig. 4? A-C). The south-western and central fringes of the Escarpment are noted to experience the highest Rx1day but lower at the upper parts (North). The trend is similar for both maximum 3-day and 5-day precipitation.

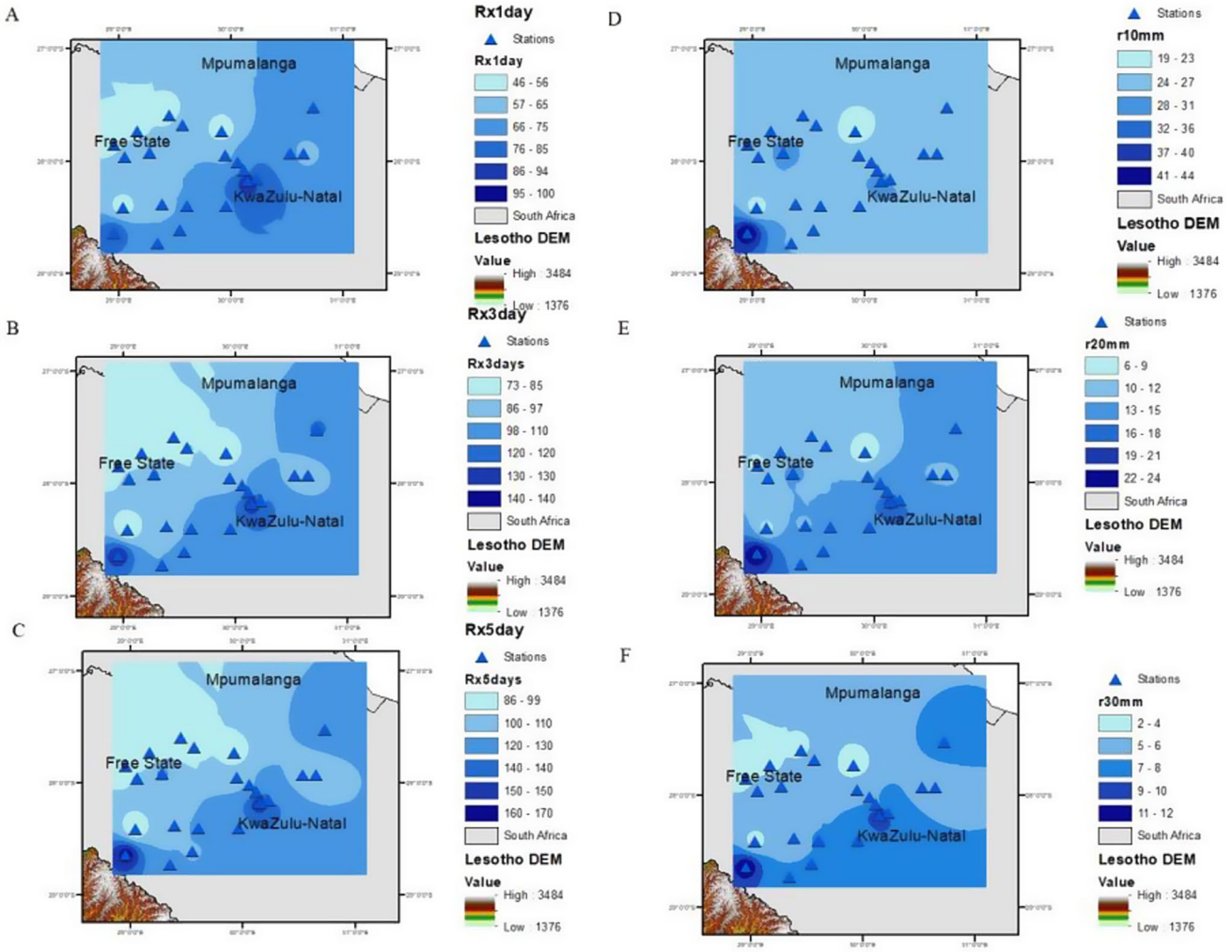

Fig. 4 Spatial pattern of precipitation indices, namely Rx1day (**A**), Rx3day (**B**), Rx5day (**C**), R10 mm (**D**), R20 mm (**E**), and R30 mm (**F**) over the Enkangala Escarpment during the period 1961–2021

3.3.2 Threshold indices

The three threshold indices considered for this study are R10 mm, R20 mm, and R30 mm for assessing heavy, very heavy, and extremely heavy precipitation days. The spatial presentations of these indices over the study area are illustrated in Fig. 4 (D-F). The average annual frequency of heavy rainfall ranges from 19 to 44 days for R10 mm across the area of interest. Moreover, the observed frequency for R20 mm varies between 6 and 24 days, while the extreme precipitation days range between 2 and 12 days. For R10 mm, the locations with the highest frequency of occurrence follows a southwest to northeast alignment along the escarpment, peaking at Cavern Farm station, close to the border with Lesotho. For R20 mm the highest numbers of 22–24 were similarly recorded in the southwestern part of the Enkangala Escarpment, including at Cavern Farm station. The northwest parts of the Enkangala escarpment experience less heavy rainfall days of 10–12 per year. Along the central Enkangala Escarpment, stations recorded, on average, 3–15 days of very heavy rainfall, with somewhat higher rainfall at Bergville, Dundee, Elandslaagte, and Glencoe (19–21 days per year). The results show a similar distribution of extreme precipitation as reported by Engelbrecht et al. (2015). For R30 mm, the lowest frequencies similarly occur over the plateau, peak along the south-eastern part of the Enkangala Escarpment, and are relatively high over KwaZulu-Natal east of the mountains (Fig. 4E).

Other threshold indices analysed are PRCPTOT and the SDII, which were calculated and annually averaged over the same period over the study area. The PRCPTOT varies from 620 to 1360 mm (Fig. 5G). Its spatial pattern resembles that of total precipitation being lower over the

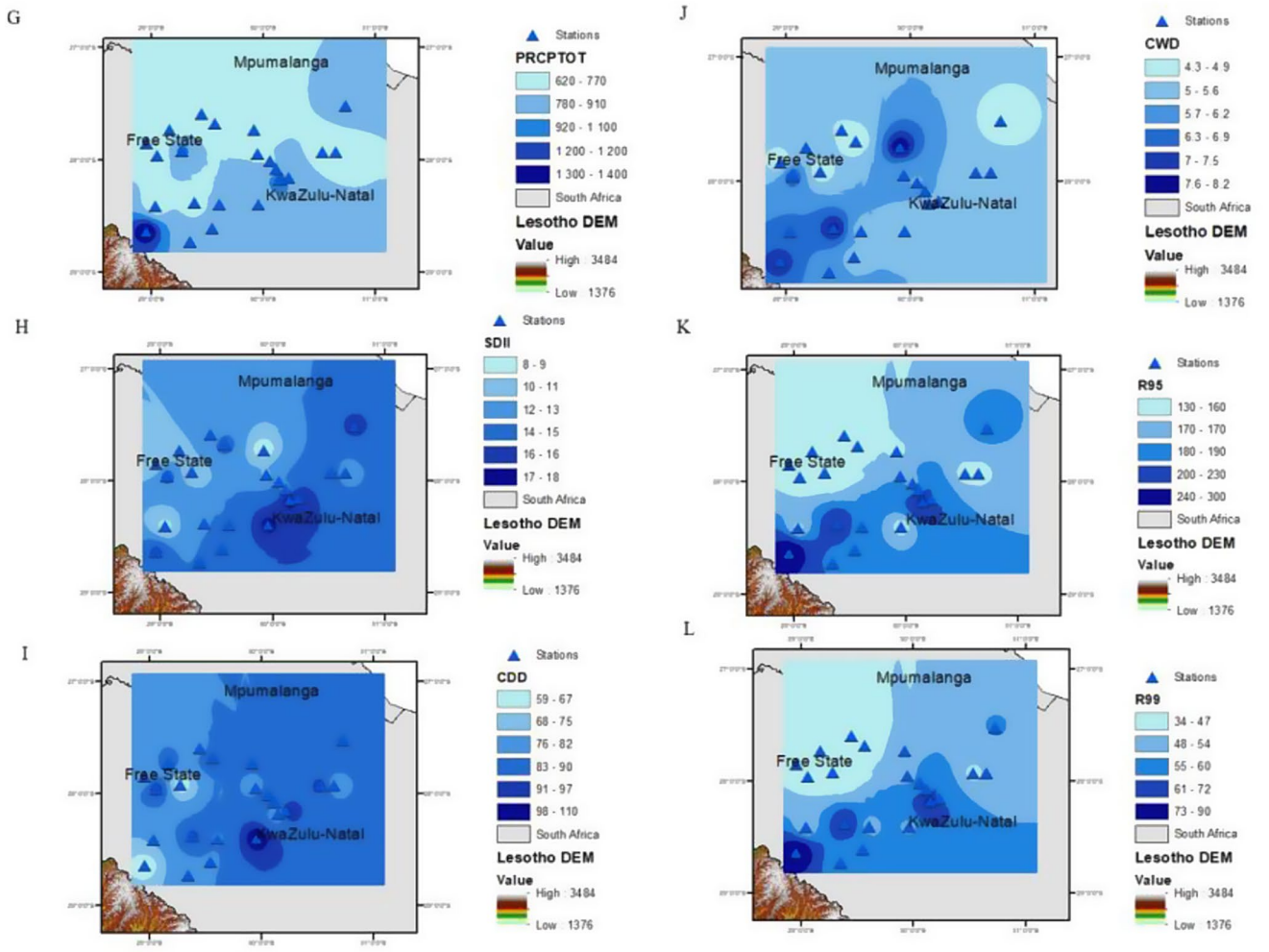

Fig. 5 Spatial distribution of precipitation indices PRCPTOT (**G**), SDII (**H**), CDD (**I**) and CWD (**J**), R95 (**K**), and R99 (**L**) over the Enkangala Escarpment, averaged for the period 1961–2021

plateau and higher along the escarpment and eastwards into the KwaZulu-Natal Province. The result are captured in the PRCPTOT maxima which spanned over the complex terrain of eastern part of South Africa, along the Inter-tropical Convergence Zone (ICTZ)(Pinto et al. 2016). The north-eastern and central Enkangala Escarpment has PRCPTOT values ranging from 620 to 770 mm per annum, lower than along the southwestern part of the escarpment along the Enkangala Escarpment, SDII intensities are highest in the central part around the Elandslaagte and Glencoe stations, with intensities of 17 and 18 mm/day (Fig. 5H).

3.3.3 Duration indices

The duration indices used are the consecutive dry days (CDD) and consecutive wet days (CWD) indices, for which annual average values were calculated for the Enkangala Escarpment region over the period 1961 to 2021 (Fig. 5I-J). The CWD has a frequency range of 4–8 days, with peak values along the southwestern and central Enkangala escarpment stations around the southwestern part (Cavern Farm and Sterkfontein) and the central region station of Van Reenen of the Enkangala Escarpment have the highest CWD. CDD frequencies are substantial, ranging between 59 and 110 days over the area of interest (Fig. 5I), as a reflection of the dry winters occurring in the subtropics.

3.3.4 Percentile-based indices

The R95p and R99p indices represent very wet and extremely wet days. These are the rainfall amounts that fall above the 95th and 99th percentiles of the distribution. The range of the R95p across the area of interest is 130 to 300 mm, while R99p ranges between 34 and 90 mm (Fig. 5, K and L). The north-eastern part of the Enkangala Escarpment exhibits the lowest values of R95p, namely

130–160 mm. Higher values have been recorded over the central escarpment, with R95p peaking over the south-western escarpment with the Cavern station having a value above 300 mm. The pattern of precipitation R95p is like that of PRCPTOT, showing a decrease from east to the very dry region in the west, Some central escarpment stations (Hattingspruit, Kingsley and Van Reenen) have values above 200 mm. The R99p spatial distribution shows a similar pattern.

3.4 Analysis of trends in extreme precipitation indices

Trends in the extreme precipitation indices are explored through the TFPWMK-statistics and field significance. The TFPWMK was used, and the results are shown in Figs. 6 and 7. Table 4 presents the summaries of the indices and their statistical significance for the different stations and the related field significance.

In the case of threshold indices of R10 mm, most stations show a non-significant decreasing trend for the 15 stations, which represents 68.2% of the total stations. Three stations, Chelmsford, Dundee and Verkykerskop, show a significantly decreasing trend (SD), whilst four stations show non-significant increasing trends (NSI) (Table 4). In comparison, R20 mm and R30 mm each have six stations which show NSD trends, all the other stations show variable trends, and these details can be seen in Table 4. The R30 mm index over the Enkangala Escarpment for the period 1961–2021 showed that 36% of stations had non-significantly increasing (NSI) trends. The field significance test over the Enkangala Escarpment for R10 mm shows an overall significantly decreasing trend, while R20mm and R30 mm show an overall significantly increasing trend (Table 4).

For the Rx1day extreme precipitation index, eight stations have SI trends. None of the stations exhibit SD, but nine stations have NSI trends, and five stations exhibit NSD trends. The field significance test shows a significantly increasing trend for the Rx1day index (Table 4). Similarly, for the Rx3day indices there are no stations with significantly decreasing trends. Rx3day have five

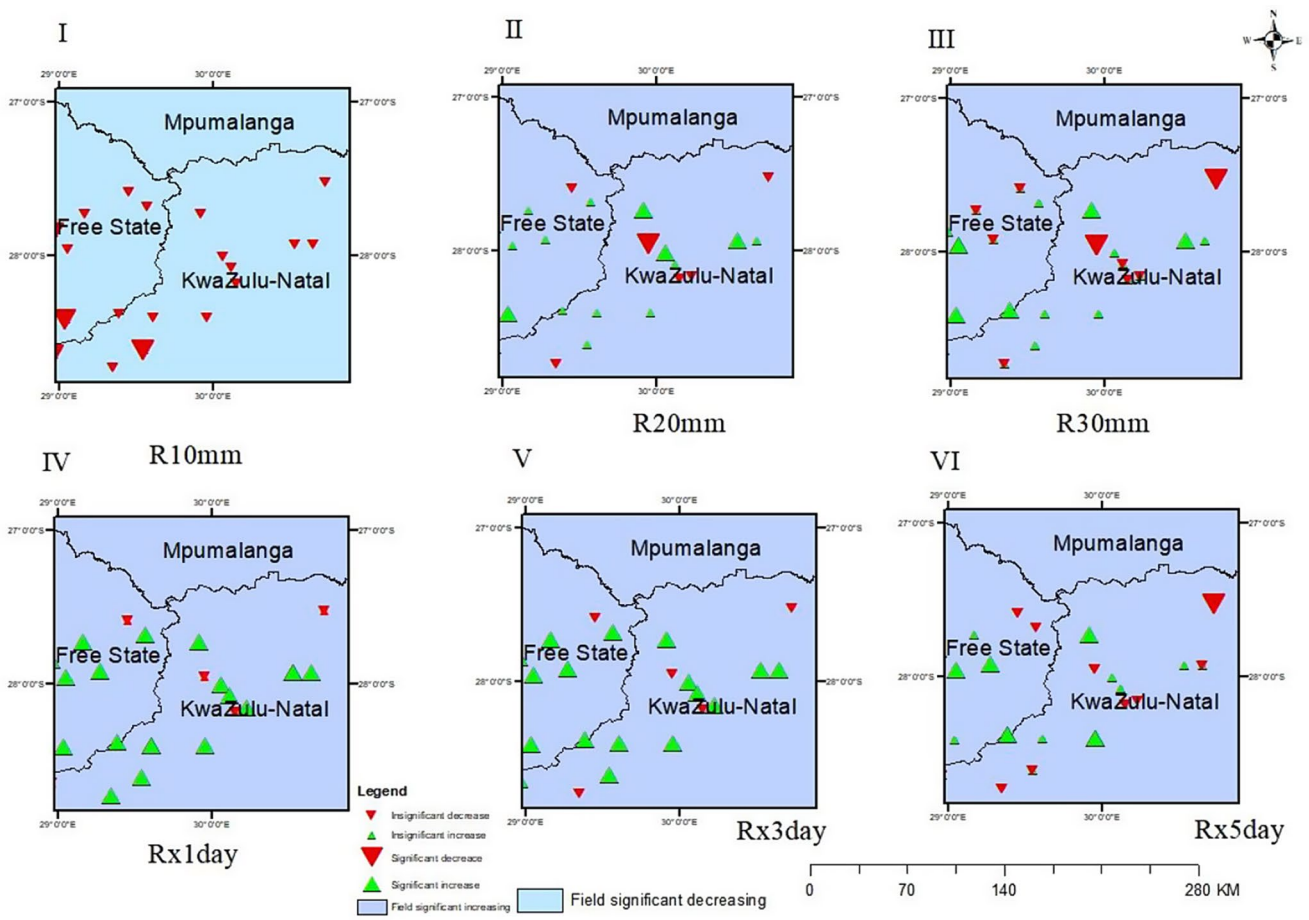

Fig. 6 Trends in precipitation indices over the Enkangala escarpment during the period 1961–2021 for R10mm (**I**), R20mm (**II**), R30mm (**III**), Rx1day (**IV**), Rx3day (**V**) and Rx5day (**VI**)

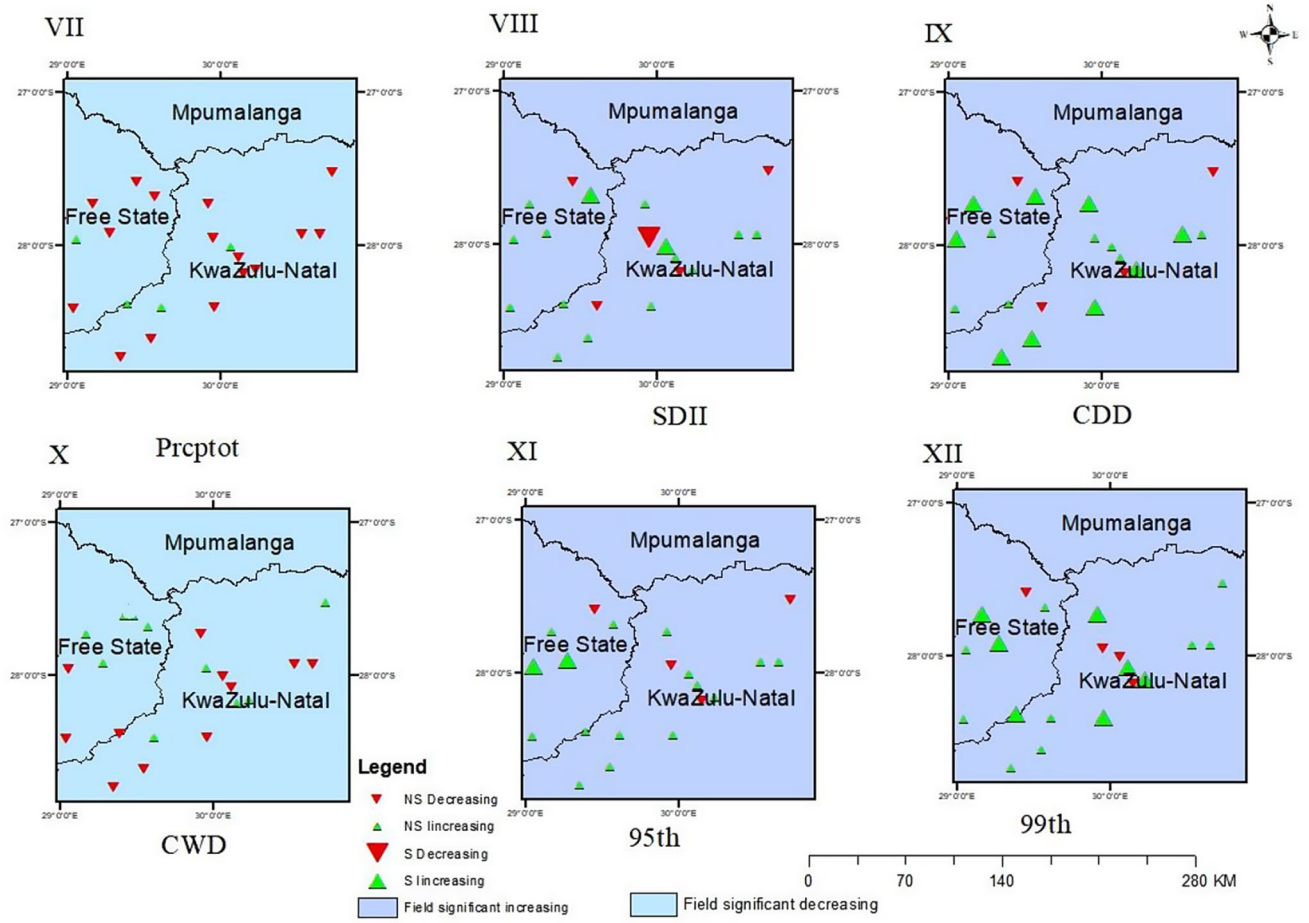

Fig. 7 Trends in precipitation indices over the Enkangala escarpment during the period 1961–2021 for PRCPTOT (**VII**), SDII (**VIII**), CDD (**IX**), CWD (**X**), R95p (**XI**) and R99p (**XII**)

Table 4 Summarized station trends in precipitation indices over the Enkangala escarpment

Indices	Trend Analysis	SI	SD	NSI	NSD	Field Significance test
SDII	TFPWMK	13	4	4	1	Significantly Increasing
Rx5day	TFPWMK	4	1	8	9	Significantly Increasing
Rx3day	TFPWMK	3	0	14	5	Significantly Increasing
Rx1day	TFPWMK	8	0	9	5	Significantly Increasing
CDD	TFPWMK	9	0	8	5	Significantly Increasing
CWD	TFPWMK	2	10	4	6	Significantly Decreasing
R10mm	TFPWMK	0	3	4	15	Significantly Decreasing
R20mm	TFPWMK	4	1	11	6	Significantly Increasing
R30mm	TFPWMK	6	2	8	6	Significantly Increasing
R95p	TFPWMK	7	1	10	4	Significantly Increasing
R99p	TFPWMK	7	0	10	5	Significantly Increasing
PRCPTOT	TFPWMK	0	0	4	17	Significantly Decreasing

stations (Bergville, Chelmsford, Glencoe, Martin and Tygerfontein) with NSD trends (Fig. 6). For the Rx5day index, nine stations, which represent 40.9% of the stations have NSD trends. For Rx3day, only three stations (Elandslaagte, Newcastle and Warden-SK) were reported to have significantly increased trends. Overall, the field significance shows a significantly increasing trend in annual total wet day precipitation. For the Rx5day index there is only one station with a significantly decreasing trend. There are eight stations with NSI trends. Precipitation increased significantly at four stations. (Elandslaagte, Newcastle, Verkykerskop and Warden-SK). The Rx3day and Rx5day field significance tests show a significantly increasing trend in annual total wet day precipitation.

The total annual precipitation PRCPTOT trends, for the period between 1961 and 2021, for the Enkangala Escarpment exhibits NSD trends for 17 stations, which represents 77% of the total stations (Table 4). Four stations (Cavern Farm, Dannhauser, Moorside and Warden_SK) show a non-significantly increasing trends of total annual precipitation. The PRCTOT field significance test shows a significantly decreasing trend (Fig. 7). The simple daily intensity index shows, that using 13 stations, represents 63.6% of the total stations, with the most varied significantly increasing trends. In addition, there are four stations (Chelmsford, Glencoe, Marthinusdrift and Tygerfontein) where the SDII shows SD trends, with four other stations showing NSI trends. Finally, only one station (Mooreside), with an NSD trend was detected (Fig. 7 VIII). The field significance test shows a significantly increasing trend for the SDII (Table 4).

For CDD, eight stations which represents 36.4% of the total stations, show significantly increasing trends. None of the stations show an SD trend for the CDD index, but five stations (Glencoe, Marthinusdrift, Mooreside, Tygerfontein and Warden-Heritage) have NSD trends. The field significance test for CDD showed a significant increasing trend.

Two stations (Glencoe and Tygerfontein) show significantly increasing trends in CWD, whilst, ten stations show significantly decreasing trends, four stations show NSI, and six stations show non-significantly decreasing trends (Cavern Farm, Elandslaagte, Martin, Rocco, Van Reenen, Warden-Heritage.

For R95p and R99p there are seven station that show significantly increasing trends. Glencoe is the only station with a significantly decreasing trend for R95p while none exists for the R99p index. Each of the indices R95p and R99p have 10 stations each with NSI trends, R95p has four stations with NSD, while R99p has five stations (Cavern Farm, Chelmsford, Danhauser, Glencoe and Tygerfontein) with NSD trends. The field significance test over the Enkangala Escarpment for R95p and R99p shows a significant positive trend (Fig. 7 XII).

3.5 Changes in precipitation indices

The entire period was split into two distinct time slices namely, 1961–1991 and 1992–2021, while the changes between the two periods were evaluated for detecting the changes in extreme precipitation events. This allows us to have an equal number of years (30 years) which is the recommended duration for reliable climate projections. The change in the precipitation regime is indicated by the average of each index value across all stations. The variation in the precipitation regime is indicated by the mean of each index value across all the stations.

As shown in Fig. 8, the 9 mm threshold index shows a slight decline by approximately −1.8 on the Escarpment's north-western flank. In comparison, the most significant positive change of 3 mm is prominent along the Escarpment's eastern flank. The 20 mm and 30 mm indices have decreased across the Escarpment except in the north-eastern area. The maximum negative change is found around Newcastle (-4 and −2.6 mm).

In contrast, the maximum increase for the 20 and 30 mm indices over the Enkangala escarpment is found in Marthinusdrift (3.3 mm) and Chelmsford (1.2 mm), respectively. The spatial distribution of heavy and severe rainfall is similar. The Rx1day and Rx3day changes are similar in their spatial distribution but differ spatially from the Rx5day distribution. The Rx1day, Rx3day and Rx5day have a maximum negative change of (-27.1, -27.5 and −29.1 mm), while their maximum positive change at Glencoe (12.6 mm) and Marthinusdrift (123.4 mm), respectively (Fig. 8).

In comparison, PRCPTOT show a non-uniform change, which decreased significantly from the north-western to the south-eastern area, except for the north-eastern portion of the Enkangala Escarpment. The SDII has significantly increased from the central to the northern area of the study area. The maximum change is approximately 4.5 mm/day, while the negative change is -4.7 mm/day (Fig. 9). The CDD has decreased across the Escarpment except for the area around the southwest. CDD showed the most significant increased change of about 86 days. Whereas for CWD, the change was reversed, i.e., a significant and negative change was noticed in the Escarpment's southwestern and central areas. The broadest range of positive changes in R95p and R99p was observed along the north-eastern to southwest gradient. The maximum positive change was found around Glencoe (70.6), indicating an increase in wet days. The findings in this research are consistent with reports by Engelbrecht et al. (2015).

3.6 Relationship between extreme precipitation and MAP

Previous research has demonstrated a strong correlation between mean annual and extreme precipitation. The correlation coefficients between the 12 precipitation indices and the Mean Annual Precipitation (MAP) from 1961 to 2021 are presented in Table 5 The MAP positively correlates with all the extreme precipitation indices except for CDD (-31.4) and is not significant from 1961 to 2021 in the Enkangala Escarpment. The indices not significantly associated with MAP are CDD, CWD and SDII. R95 and R99 are the only indices that correlate with MAP at a 0.05 significance level, while the rest of the significantly correlated indices were at a 0.01 significance level. Rx3days has the highest correlation

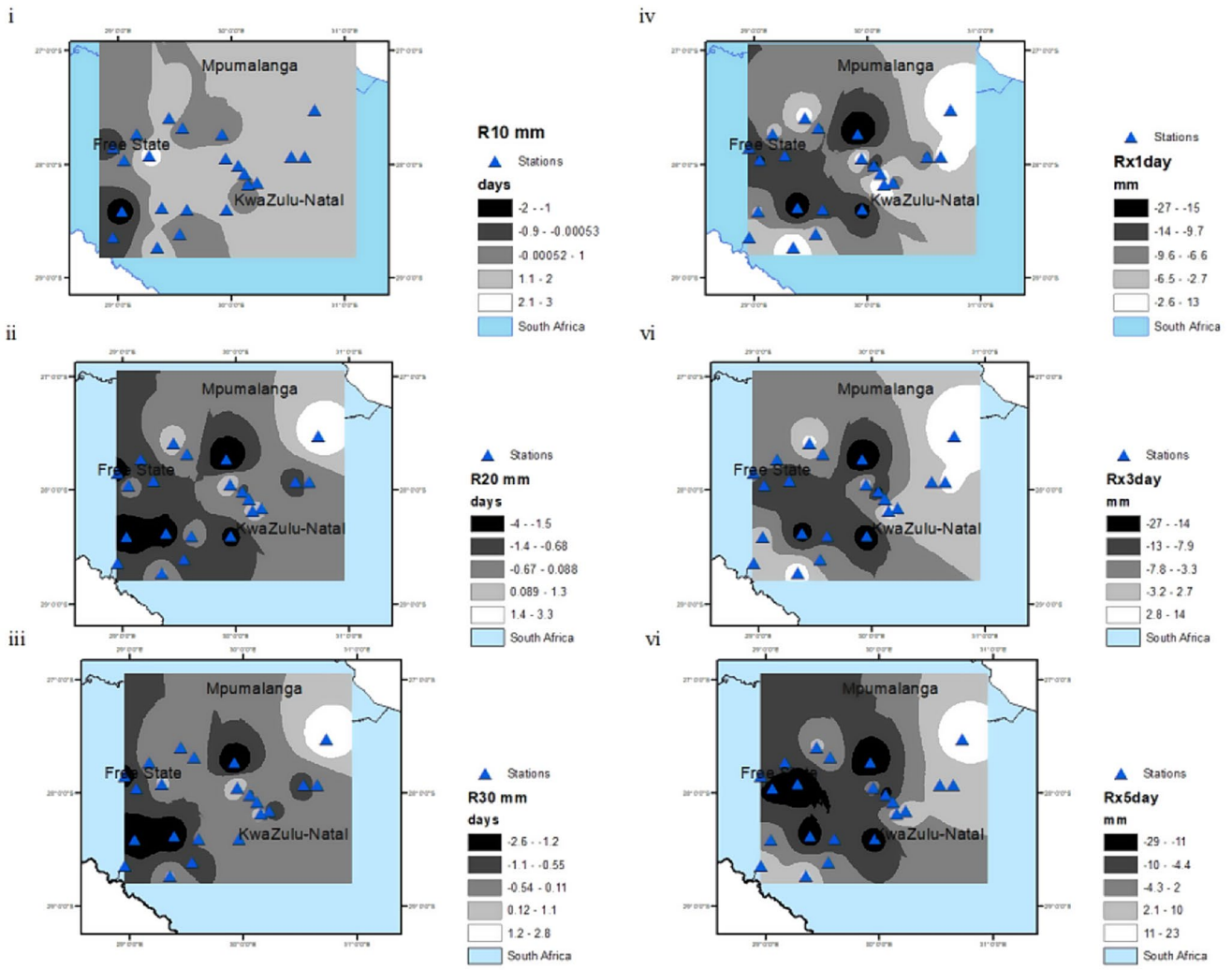

Fig. 8 The spatial distribution of changes in extreme event indices over the Enkangala Escarpment during 1961–2021, for R10mm (**i**), R20mm (**ii**), R30mm (**iii**), Rx1day (**iv**), Rx3day (**v**) and Rx5day (**vi**)

coefficient (r=0.89), and the lowest positive correlation is R95 (r=0.56) at a 0.05 significance level. The correlation coefficients of MAP with PRCPTOT, R10 mm, R20 mm, R30 mm, Rx1day, Rx3day and Rx5day were more significant than 0.70 (Table 5).

4 Conclusion

Our analysis has detected an overall statistically significant decrease (in terms of field significance) in rainfall totals over the Enkangala Escarpment. This trend occurs in association with a statistically significant decrease in the number of days with rainfall totals higher than 10 mm (R10mm index). Moreover, statistically significant increases in the number of consecutive dry days (CDD index) and decreases in consecutive wet days (CWD index) were consistently detected. These findings are generally consistent with climate model simulations that point towards more subsidence and general decreases in rainfall over southern Africa in a warmer world (Engelbrecht et al. 2009, 2015; Engelbrecht et al., 2022; Giorgi, 2014). A similar conclusion of decreasing trends in rainfall trends over the larger region of eastern South Africa was reached by MacKellar et al. (2014), and the IPCC Sixth Assessment Report similarly assessed that decreasing rainfall totals over eastern South Africa is a trend that can already be detected (Ranasinghe et al. 2021).

However, it is not only rainfall totals that are changing over the Enkangala Escarpment, our results reveal that it is also the nature of rainfall that is changing. Field significance tests show a statistically significant increase for almost all extreme precipitation indices: R20 mm, R30 mm, R95p, R99p, Rx1day, Rx2day, Rx3day and SDII. The only exceptions are R10 mm and CWD, which show a decreasing trend in frequency in field significance

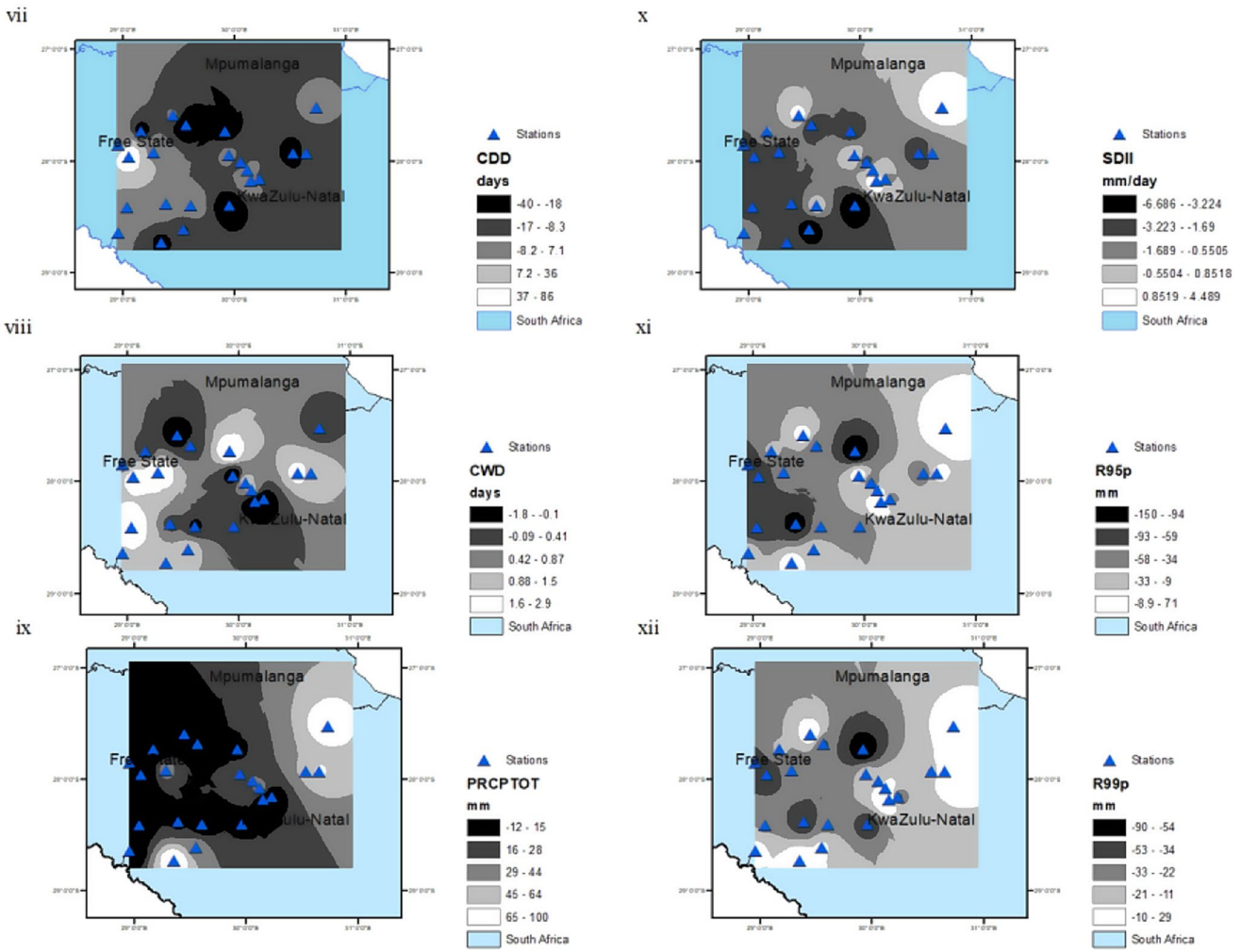

Fig. 9 The spatial distribution of changes in extreme event indices over Enkangala Escarpment during 1961–2021for PRCPTOT (**vii**), SDII (**viii**), CDD (**ix**), CWD (**x**), R95p (**xi**) and R99p (**xii**)

Table 5 The correlation coefficient (r) and level of significance between MAP and Extreme Precipitation indices (0.05 => *)

Indices	*R*	Sig level
SDII	0.44	
CDD	-0.31	
CWD	0.36	
PRCPTOT	-0.77	**
R10m	0.8	**
R20m	0.79	**
R30m	0.72	**
R95	0.56	*
R99	0.65	*
Rx1day	0.71	**
Rx3day	0.89	**
Rx5day	0.87	**

tests. One may speculate that the convective rainfall events that bring rainfall over the Enkangala escarpment have become more intense (rainfall totals shifting from the R10 mm threshold to the R20 mm and R30 mm thresholds), but that fewer such events occur (increase in CDD and decrease in CWD). That is, rainfall totals are decreasing, and it is raining less frequently, but when it does rain it is with increased intensity. Our findings of general increases in precipitation extremes are qualitatively consistent with those of MacKellar et al. (2014) and McBride (2022) for eastern South Africa, and with the assessment of the IPCC AR6 for eastern Southern Africa (Ranasinghe et al. 2021).

Should these trends persist in a warming climate, challenges for adaptation will be substantial. The agriculture sector will have to adapt towards decreasing rainfall trends, which in combination with increasing temperatures will result in reduced soil-moisture availability. At the same time, more intense rainfall events will carry higher risks of inducing soil erosion. In terms of water management, decreasing rainfall overall may be compensated by increased run-off from the increase in extreme rainfall events. However, even under such a scenario,

there is the risk of increasing soil erosion and increased sedimentation in dams.

Acknowledgements The authors are grateful to the South Africa Weather Services (SAWS) for providing datasets for the research. We also acknowledge the support from Forestry South Africa (FSA) and the NRF for funding (FSA2020 and FSA2023).

Author contributions Hadisu Bello Abubakar: Conceptualization, Data acquisition, Formal analysis, The investigation, Methodology, Visualization, Writing – original draft, Scholes MC: Writing, Conceptualisation, Resources, Engelbrecht, FA: Software, Writing – review & editing.

Funding Open access funding provided by University of the Witwatersrand.
This work was supported by Forestry South Africa (SA Forestry), Grant numbers (FSA2020).

Data availability Data are available on resonable request.

Declarations

Competing interests The authors declare no competing interests.

References

Abba Omar S, Abiodun BJ (2017) How well do CORDEX models simulate extreme rainfall events over the East Coast of South Africa? Theoretical and applied climatology 128:453–464

Adeyeri O, Laux P, Ishola k Zhou, w., Balogun, i., adeyewa, z. & kunstmann, h. 2022. Homogenising meteorological variables: impact on trends and associated climate indices. J Hydrol, 607, 127585

Almazroui M, Şen Z (2020) Trend analyses methodologies in hydrometeorological records. Earth Syst Environ 4:713–738

Anekwe IMS, Zhou H, Mkhize MM, Akpasi SO (2023) Effects of climate change on agricultural production in South Africa. International Journal of Climate Change: impacts & responses 15(2)

Bartolini G, Betti G, Gozzini B, Iannuccilli M, Magno R, Messeri G, Spolverini N, Torrigiani T, Vallorani R, Grifoni D (2022) Spatial and temporal changes in dry spells in a Mediterranean area: Tuscany (central Italy), 1955–2017. Int J Climatol 42:1670–1691

Bopape M-JM, Engelbrecht FA, Maisha R, Chikoore H, Ndarana T, Lekoloane L, Thatcher M, Mulovhedzi PT, Rambuwani GT, Barnes MA (2022) Rainfall Simulations of High-Impact Weather in South Africa with the Conformal Cubic Atmospheric Model (CCAM). *Atmosphere*, 13, 1987

Branca G, Arslan A, Paolantonio A, Grewer U, Cattaneo A, Cavatassi R, Lipper L, Hillier J, Vetter S (2021) Assessing the economic and mitigation benefits of climate-smart agriculture and its implications for political economy: a case study in Southern Africa. J Clean Prod 285:125161

Bruinsma J (2017) World agriculture: towards 2015/2030: an FAO study. Routledge

Charifi Bellabas S, Benmamar S, Dehni A (2021) Study and analysis of the streamflow decline in North Algeria. J Appl Water Eng Res 9:20–44

Citakoglu H, Minarecioglu N (2021) Trend analysis and change point determination for hydro-meteorological and groundwater data of Kizilirmak basin. Theoret Appl Climatol 145:1275–1292

Dedekind Z, Engelbrecht FA, Van der Merwe J (2016) Model simulations of rainfall over southern Africa and its eastern escarpment. Water SA 42(1):129–143

Douris J, Kim G (2021) The Atlas of Mortality and Economic Losses from Weather, Climate and Water Extremes (1970–2019)

Dunkerley D (2021) The case for increased validation of rainfall simulation as a tool for researching runoff, soil erosion, and related processes. CATENA 202:105283

Engelbrecht CJ, Engelbrecht FA (2016) Shifts in Köppen-Geiger climate zones over southern Africa in relation to key global temperature goals. Theoret Appl Climatol 123:247–261

Engelbrecht FA, Monteiro P (2022) The IPCC assessment report six working group 1 report and southern Africa: reasons to take action. South Afr J Sci 117:1–7

Engelbrecht F, Rautenbach DW, Mcgregor J, Katzfey J (2002) January and July climate simulations over the SADC region using the limited-area model DARLAM. WATER SA-PRETORIA- 28:361–374

Engelbrecht F, Mcgregor J, Engelbrecht C (2009) Dynamics of the Conformal-Cubic Atmospheric Model projected climate-change signal over southern Africa. Int J Climatology: J Royal Meteorological Soc 29:1013–1033

Engelbrecht F, Adegoke J, Bopape M-J, Naidoo M, Garland R, Thatcher M, Mcgregor J, Katzfey J, Werner M, Ichoku C (2015) Projections of rapidly rising surface temperatures over Africa under low mitigation. Environ Res Lett 10:085004

Garba I, Abdourahamane ZS (2023) Extreme rainfall characterisation under climate change and rapid population growth in the city of Niamey, Niger. Heliyon 9(2)

Giorgi F, Coppola E, Raffaele F, Diro GT, Fuentes-Franco R, Giuliani G, Mamgain A, Llopart MP, Mariotti L, Torma C (2014) Changes in extremes and hydroclimatic regimes in the CREMA ensemble projections. Clim Change 125:39–51

Gu X, Zhang Q, Singh VP, Shi P (2017) Changes in magnitude and frequency of heavy precipitation across China and its potential links to summer temperature. J Hydrol 547:718–731

Guijarro JA (2014) Quality control and homogenization of climatological series. *Eslamian S*

Guijarro JA (2018) Homogenization of climatic series with Climatol. *Reporte técnico State Meteorological Agency (AEMET), Balearic Islands Office, Spain*

Guijarro J (2019) Climatol: Climate Tools (series homogenization and derived products). *R package version*, 3

Guijarro JA, López JA, Aguilar E, Domonkos P, Venema VK, Sigró J, Brunet M (2023) Homogenization of monthly series of temperature and precipitation: benchmarking results of the MULTITEST project. International Journal of Climatology 43(9):3994–4012

Hoegh-Guldberg O, Jacob D, Bindi M, Brown S, Camilloni I, Diedhiou A, Djalante R, Ebi K, Engelbrecht F, Guiot J (2018) Impacts of 1.5 C global warming on natural and human systems. *Global warming of 1.5° C.*

Hoegh-Guldberg O, Jacob D, Taylor M, Guillén Bolaños T, Bindi M, Brown S, Camilloni IA, Diedhiou A, Djalante R, Ebi K (2019)

The human imperative of stabilizing global climate change at 1.5 C. Science 365:eaaw6974

Jin S, Ma Y, Huang Z, Huang J, Gong W, Liu B, Wang W, Fan R, Li H (2023) A comprehensive reappraisal of long-term aerosol characteristics, trends, and variability in Asia. Atmospheric Chemistry and Physics 23(14):8187–8210

Karki R, Hasson SU, Schickhoff U, Scholten T, Böhner J (2017) Rising precipitation extremes across Nepal. Climate 5:4

Kruger A, Sekele S (2013) Trends in extreme temperature indices in South Africa: 1962–2009. Int J Climatol 33:661–676

Lee JY, Marotzke J, Bala G, Cao L, Corti S, Dunne JP, Engelbrecht F, Fischer E, Fyfe JC, Jones C, Maycock A (2021) Future global climate: scenario-based projections and near-term information. In Climate change 2021: the physical science basis. Contribution of working group I to the sixth assessment report of the intergovernmental panel on climate change (pp. 553–672). Cambridge University Press

Mackellar N, New M, Jack C (2014) Observed and modelled trends in rainfall and temperature for South Africa: 1960–2010. South Afr J Sci 110:1–13

Mcbride S-L (2022) Afterlives of land dispossession and patterns of Climate Change: intersections in South African contemporary art. J South Afr Stud 48:503–525

Montero-Martínez MJ, Andrade-Velázquez M (2022) Effects of Urbanization on Extreme Climate indices in the Valley of Mexico Basin. Atmosphere 13:785

Naidoo S (2022) Commentary on the contribution of Working Group III to the Sixth Assessment Report of the Intergovernmental Panel on Climate Change. South Afr J Sci 118:1–4

Naidoo S, Davis C, Van Garderen EA (2013) Forests, rangelands and climate change in southern Africa. *Forests and climate change working paper*, 12

Nel JL, Le Maitre DC, Roux DJ, Colvin C, Smith JS, Smith-Adao LB, Maherry A, Sitas N (2017) Strategic water source areas for urban water security: making the connection between protecting ecosystems and benefiting from their services. Ecosyst Serv 28:251–259

Nel W, Sumner PD (2006) Trends in rainfall total and variability (1970–2000) along the KwaZulu-Natal Drakensberg foothills. South African Geographical Journal 88(2):130–137

Nhemachena C, Nhamo L, Matchaya G, Nhemachena CR, Muchara B, Karuaihe ST, Mpandeli S (2020) Climate change impacts on water and agriculture sectors in Southern Africa: threats and opportunities for sustainable development. Water 12:2673

Olabanji MF, Ndarana T, Davis N (2020) Impact of climate change on crop production and potential adaptive measures in the olifants catchment, South Africa. Climate 9:6

Onaolapo TF, Okello TW, Adelabu SA, Adagbasa EG (2022) Change in the Urban Landscape of the Drakensberg Mountain Region, South Africa: a case study of Phuthaditjhaba. Mt Res Dev 42:R63–R74

Palharini RSA, Vila DA, Rodrigues DT, Palharini RC, Mattos EV, Pedra GU (2021) Assessment of extreme rainfall estimates from satellite-based: Regional analysis. Remote Sens Applications: Soc Environ 23:100603

Petrow T, Merz B (2009) Trends in flood magnitude, frequency and seasonality in Germany in the period 1951–2002. J Hydrol 371:129–141

Pinto I, Lennard C, Tadross M, Hewitson B, Dosio A, Nikulin G, Panitz H-J, Shongwe ME (2016) Evaluation and projections of extreme precipitation over southern Africa from two CORDEX models. Clim Change 135:655–668

Punge HJ, Bedka KM, Kunz M, Bang SD, Itterly KF (2023) Characteristics of hail hazard in South Africa based on satellite detection of convective storms. Natural Hazards and Earth System Sciences 23(4):1549–1576

Quintero F, Villarini G, Prein AF, Zhang W, Krajewski WF (2022) Discharge and floods projected to increase more than precipitation extremes. Hydrol Process 36:e14738

Ran Q, Wang F, Gao J (2019) Modelling effects of rainfall patterns on runoff generation and soil erosion processes on slopes. Water 11:2221

Ranasinghe R, Ruane AC, Vautard R, Arnell N, Coppola E, Cruz FA, Dessai S, Islam S, Rahimi A, M., Carrascal DR (2021) Climate change information for regional impact and for risk assessment

RENARD B, LANG M (2007) Use of a gaussian copula for multivariate extreme value analysis: some case studies in hydrology. Adv Water Resour 30:897–912

Risser MD, Wehner MF, O'brien JP, Patricola CM, O'brien TA, Collins WD, Paciorek CJ, Huang H (2021) Quantifying the influence of natural climate variability on in situ measurements of seasonal total and extreme daily precipitation. Clim Dyn 56:3205–3230

Sevruk B, Ondrás M, Chvíla B (2009) The Wmo precipitation measurement intercomparisons. Atmos Res 92:376–380

Sierks MD (2022) Distinctive impacts of Extreme warm season precipitation and climate change on the Vulnerable Water resources of the Southwestern United States. University of California, San Diego

Steinschneider S, Brown C (2013) A semiparametric multivariate, multisite weather generator with low-frequency variability for use in climate risk assessments. Water Resour Res 49:7205–7220

Strauss J, Swanepoel P, Laker MC, Smith H (2021) Conservation agriculture in rainfed annual crop production in South Africa. South Afr J Plant Soil 38:217–230

Tan X, Gan TY, Shao D (2017) Effects of persistence and large-scale climate anomalies on trends and change points in extreme precipitation of Canada. J Hydrol 550:453–465

Tan X, Wu Y, Liu B, Chen S (2020) Inconsistent changes in global precipitation seasonality in seven precipitation datasets. Clim Dyn 54:3091–3108

Taylor SJ, Ferguson JWH, Engelbrecht FA, Clark VR, Van Rensburg S, Barker N (2016) The drakensberg escarpment as the great supplier of water to South Africa. In Developments in Earth Surface Processes, Vol. 21, Elsevier, pp. 1–46

Trenberth KE (2011) Changes in precipitation with climate change. Climate Res 47:123–138

Van Der Walt AJ, Fitchett JM (2021) Exploring extreme warm temperature trends in South Africa: 1960–2016. Theoret Appl Climatol 143:1341–1360

Yin J, Guo S, Gentine P, Sullivan SC, Gu L, He S, Chen J, Liu P (2021) Does the hook structure constrain future flood intensification under anthropogenic climate warming? Water Resour Res, 57, e2020WR028491.

Yue S, Wang CY (2002) Regional Streamflow trend detection with consideration of both temporal and spatial correlation. Int J Climatology: J Royal Meteorological Soc 22:933–946

Yue S, Pilon P, Phinney B (2003) Canadian streamflow trend detection: impacts of serial and cross-correlation. Hydrol Sci J 48:51–63

Zeder J, Fischer EM (2020) Observed extreme precipitation trends and scaling in Central Europe. Weather Clim Extremes 29:100266

Zhao L, Fang Q, Hou R, Wu F (2021) Effect of rainfall intensity and duration on soil erosion on slopes with different microrelief patterns. Geoderma 396:115085